AIMS Environmental Science

https://www.aimspress.com/journal/environmental

AIMS Environmental Science, 13(4): 774–796.
DOI: 10.3934/environsci.2026031
Received: 01 August 2026
Revised: 09 September 2026
Accepted: 11 September 2026
Published: 20 September 2026

*Research article*

# Manufacturing-attributed generation carbon intensity of monocrystalline silicon photovoltaic modules in China under production–use spatial coupling

**Yaokuan Peng[1], Siyuan Chen[1], Yao Tong[1], Xinyuan Jin[1] and Lipu Zhang[1,2,*]**

[1] School of Media Engineering, Communication University of Zhejiang, Hangzhou 310018, China
[2] National Radio and Television Administration Laboratory for Media Intelligent Communication Technology, Hangzhou 310018, China

* **Correspondence:** Email: zhanglipu@cuz.edu.cn.

**Abstract:** Photovoltaic (PV) module manufacturing footprints are typically reported per kWp, yet their interpretation changes when these burdens are allocated over lifetime electricity generation in regions with unequal solar resources. We present a parameterized life-cycle assessment (LCA) model for monocrystalline silicon PV modules linking manufacturing emissions, provincial grid factors, solar resources, technology routes, material-factor scenarios, and Monte Carlo uncertainty. Manufacturing-footprint results are reported in kg $CO_2$e/kWp, while generation-intensity outcomes are described by their relative rankings to avoid mixing different allocation bases. Built on International Energy Agency Photovoltaic Power Systems Programme (IEA PVPS) Task 12 inventories, ecoinvent 3.9.1 Cutoff material factors with the Intergovernmental Panel on Climate Change (IPCC) 2021 100-year global warming potential (GWP100), China's 2023 provincial electricity factors, and the NASA POWER 2014–2023 irradiation data, the 19.5% crystalline-silicon (c-Si) reference module yields 494.4 kg $CO_2$e/kWp under national-average manufacturing electricity. Route-specific proxies for passivated emitter and rear cell (PERC), tunnel oxide passivated contact (TOPCon), and heterojunction (HJT) modules give 446.2, 392.8, and 367.9 kg $CO_2$e/kWp, respectively, under the ecoinvent 3.9.1 Cutoff factor set. The three factor sets are the ecoinvent 3.9.1 Cutoff, China-adjusted literature, and low-carbon materials-and-power sets; their route-specific ranges are 367.9–446.2, 593.0–719.4, and 73.9–88.7 kg $CO_2$e/kWp, respectively. The production–use matrix distinguishes manufacturing-location effects from use-location solar-resource effects, while the uncertainty analysis shows that factor-set ordering is more stable than technology-route ordering. PV carbon-footprint screening should jointly disclose material factors, electricity factors, solar-resource assumptions, and technology-route parameters.

**Keywords:** carbon footprint; life cycle assessment; monocrystalline silicon photovoltaic module; provincial electricity factor; production–use spatial coupling

## Nomenclature

| | |
|---|---|
| AP | acidification potential |
| BOM | bill of materials |
| c-Si | crystalline silicon |
| CF | carbon footprint |
| CI | manufacturing-attributed generation carbon intensity |
| ECFW | freshwater ecotoxicity |
| EF | emission factor |
| EP | eutrophication potential |
| EVA | ethylene-vinyl acetate |
| GSD | geometric standard deviation |
| HJT | heterojunction technology |
| HTC | human toxicity cancer |
| HTNC | human toxicity non-cancer |
| LCA | life-cycle assessment |
| LCIA | life cycle impact assessment |
| MIR | maximum incremental reactivity |
| ODP | ozone depletion potential |
| PERC | passivated emitter and rear cell |
| PMFP | particulate matter formation potential |
| PR | performance ratio |
| PV | photovoltaic |
| PVF | polyvinyl fluoride |
| RoW | Rest of World |
| TOPCon | tunnel oxide passivated contact |
| TRACI | Tool for the Reduction and Assessment of Chemical and other environmental Impacts |

## 1. Introduction

Photovoltaic (PV) generation has low direct emissions during operation, but crystalline-silicon modules carry environmental burdens from manufacturing and, in complete system assessments, installation before they generate electricity. Polysilicon production, ingot pulling, wafer slicing, cell manufacturing, module encapsulation, glass, aluminium frames, encapsulants, and other inputs all contribute to the cradle-to-gate carbon footprint of the module. At high deployment volumes, those upstream burdens matter for climate-mitigation accounting, product carbon-footprint comparison, low-carbon procurement, and the design of photovoltaic supply chains. The issue is especially visible in countries that combine a large manufacturing capacity with a strong regional variation in electricity mix and solar resource.

Life-cycle assessment (LCA) methods for PV modules are well established under ISO 14040 and ISO 14044 [1, 2]. Product carbon-footprint quantification is further guided by ISO 14067 [3]. International Energy Agency PV Power Systems Programme (IEA PVPS) Task 12 has provided PV inventory data and the interpretation for module and system assessments [4,5]. At the module level, the

footprint includes upstream silicon production, cell processing, glass, aluminium frames, encapsulants, and module-assembly electricity. Therefore, cell processing is one stage within module manufacturing rather than a synonym for the complete module footprint. Chowdhury et al. identified aluminium and low-iron glass as important materials in PV-module circularity [6], while Müller et al. showed that the module design, manufacturing location, and inventory choice can affect the module-level LCA results [7]. Previous work has shown that silicon, cell manufacturing, glass, aluminium frames, and manufacturing electricity are common hotspots across crystalline-silicon module and cell-production inventories [8, 9]. These studies use several related functional units. A cradle-to-gate kg $CO_2$e/kWp metric compares manufacturing burdens per installed capacity, while a g $CO_2$e/kWh metric allocates those burdens over lifetime generation and is closer to climate-mitigation interpretation. Conflating these units can obscure whether a difference is caused by manufacturing emissions, module power density, or lifetime yield.

Data provenance is a second source of variation. The ecoinvent database provides standardized background inventories for materials, energy supply, and transport, but the database version, system model, allocation rule, recycled-material treatment, and geographic proxy affect both total footprints and hotspot rankings [10]. Therefore, the literature contains two related but distinct comparison problems: cell- or process-level studies may identify a process hotspot, whereas module-level studies allocate all selected module materials and processes to a common functional unit. A transparent analysis should state which object is being compared and whether installation and balance-of-system processes are included. Recent studies have highlighted geographic representativeness concerns for PV modules manufactured in China [11] and public life cycle inventory (LCI) data gaps for silicon PV [12]. A Chinese case study showed that production and installation locations can affect the life-cycle results [13], while research on module production in Mexico illustrates how globally distributed supply chains, imported cells, and transport can affect the reported footprint [14]. Therefore, for environmental reporting, a footprint value without its factor source, electricity factor, life cycle impact assessment (LCIA) method, and boundary is difficult to compare across studies or procurement thresholds.

However, spatial variation is usually treated on only one side of the calculation. Manufacturing-location electricity affects the cradle-to-gate footprint, while use-location irradiation affects the lifetime-generation denominator. Few screening studies reported these two spatial terms as a production–use matrix and then tested whether the resulting rankings were more sensitive to material-factor provenance or to cell-route assumptions. Monte Carlo propagation has been used in LCA to support environmentally preferable choices under uncertainty [15], but uncertainty in the module footprint and generation carbon intensity is still commonly discussed separately from production–use geography.

This spatial distinction matters for environmental decisions. A factory-gate module footprint reported in kg $CO_2$e/kWp can support product comparisons, but it does not show how the same module burden is distributed over lifetime generation in a low- or high-resource use region. Conversely, solar-resource ranking alone does not identify the manufacturing burden embedded in the module. Connecting the production location, material-factor provenance, and use-location generation helps clarify when low-carbon manufacturing electricity, low-carbon materials, and high solar resource reinforce each other and when they do not.

This study asks whether province-level production–use coupling changes the interpretation of

monocrystalline PV module carbon footprints, and whether uncertainty in material-factor provenance exceeds the differences among passivated emitter and rear cell (PERC), tunnel oxide passivated contact (TOPCon), and heterojunction technology (HJT) route assumptions. The analysis contributes by (i) converting cradle-to-gate kg $CO_2$e/kWp into manufacturing-attributed g $CO_2$e/kWh for 31 representative provincial cities, (ii) separating the manufacturing-location and use-location effects through a 30 by 31 production–use matrix, and (iii) testing material-factor scenarios, technology-route assumptions, and uncertainty propagation in one reproducible screening model. The aim is not to claim a complete PV power-plant LCA, but to report how data provenance, manufacturing electricity, solar resource, and the technology route jointly affect module-manufacturing carbon-footprint interpretation.

## 2. Materials and methods

### *2.1. Goal, calculation bases and system boundary*

The goal is to quantify the cradle-to-gate manufacturing carbon footprint of a monocrystalline silicon (c-Si) PV module and to show how the same module burden changes when allocated over lifetime electricity generation in different Chinese provinces. The primary functional unit for the cradle-to-gate comparison is 1 kWp of installed module capacity. The manufacturing inventory is initially calculated using an area-based reference flow of 1 m² of module and is then converted to the capacity-based functional unit. For the generation-intensity analysis, the manufacturing burden is additionally allocated over 1 kWh of the modeled lifetime electricity output. The product studied is a c-Si PV module with an aluminium frame. The manufacturing boundary is cradle-to-gate and covers the major material inputs, silicon production, ingot pulling, wafer slicing, cell manufacturing, and module encapsulation. Transport in this statement means module-level logistics and any foreground transport not already represented in the selected background activities; upstream transport embedded in an ecoinvent market or production activity remains included where that dataset provides it. Mounting structures, inverters, installation, operation and maintenance, and end-of-life treatment are outside the baseline boundary. Minor materials whose mass share and carbon contribution are both below 1% are omitted under a cutoff rule. This boundary is selected because the study aims to compare product manufacturing burdens and their generation-weighted interpretation, rather than to claim a complete PV power-plant inventory.

Two related module objects are used, as summarized in Table 1. First, a 19.5% generic c-Si reference module from the IEA PVPS inventory is used for provincial manufacturing footprints and same-province production/use results. Second, route-specific PERC, TOPCon, and HJT module proxies are used to compare technology routes and material-factor scenarios. These route-specific modules have different efficiencies, material intensities, and process-energy assumptions, so their results are not directly comparable with the 19.5% reference-module results.

**Table 1.** Modeled module objects and their use in the analysis.

| Module object | Main assumptions | Used for | Reported outputs |
|---|---|---|---|
| Generic reference module | IEA PVPS 19.5% module with national or provincial manufacturing electricity | Baseline manufacturing footprint, same-province production/use results, production–use matrix, efficiency and foreground green-electricity tests | kg $CO_2$e/kWp and manufacturing-attributed g $CO_2$e/kWh |
| Route-specific modules | PERC, TOPCon, and HJT proxies with route-specific parameters and screening-level process-energy and degradation assumptions | Technology-route comparison, material-factor scenarios, uncertainty, hotspot restructuring, decarbonization pathway | kg $CO_2$e/kWp and material-side shares |

Figure 1 summarizes the calculation and reporting bases and the included and excluded processes.

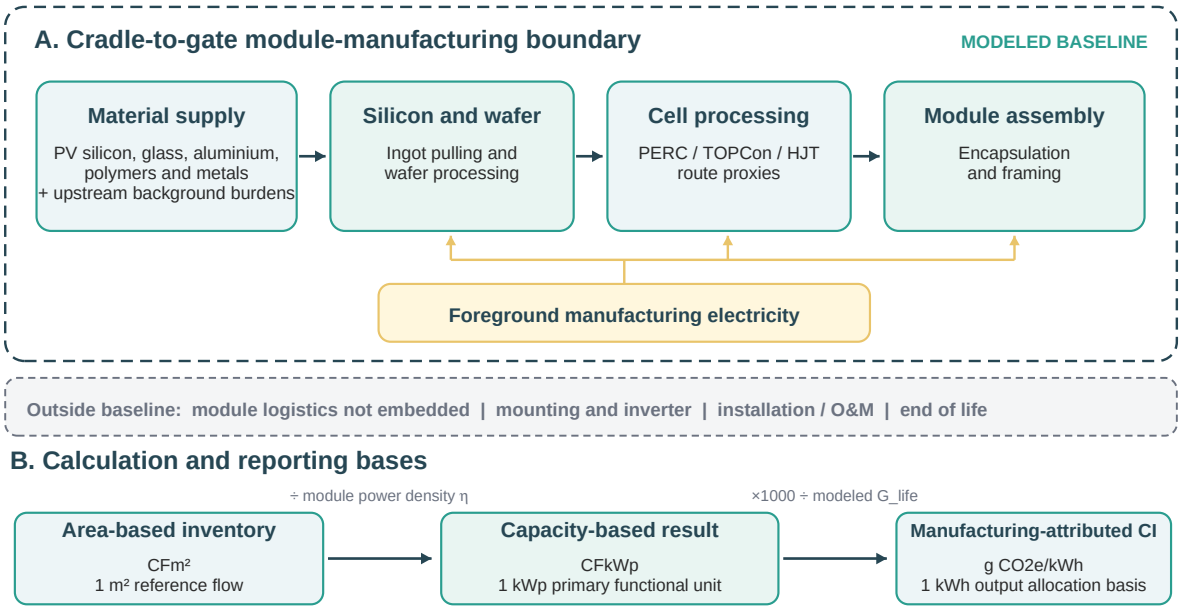



**Figure 1.** Cradle-to-gate system boundary and calculation bases used in the screening model.

### 2.2. *Data sources and parameter provenance*

The model combines public inventory, factor, and resource data, as listed in Table 2. IEA PVPS Task 12 provides the module bill of materials (BOM), default efficiency, and foreground process electricity for ingot pulling, wafer slicing, cell manufacturing, and module encapsulation [4, 5]. Solar-grade silicon is represented by an ecoinvent production-process factor whose upstream purification energy is

already included; therefore, the 49 kWh/kg silicon-purification electricity in the IEA spreadsheet is not added again [4, 5].

The baseline material factors were queried from specific ecoinvent 3.9.1 Cutoff activities and characterized using IPCC 2021 GWP100. Wernet et al. [10] is used as methodological background for the ecoinvent version 3 database and its system-model structure, rather than as the source of the individual factor values.

Foreground electricity emissions are calculated using the official 2023 national and provincial electricity $CO_2$ factors [16]. Because these factors report $CO_2$ rather than a complete $CO_2$-equivalent electricity inventory including non-$CO_2$ greenhouse gases, their combination with material-side $CO_2$e results should be interpreted as a screening approximation.

Monthly National Aeronautics and Space Administration Prediction Of Worldwide Energy Resources (NASA POWER) `ALLSKY_SFC_SW_DWN` records, meaning all-sky surface shortwave downward irradiance, were converted from monthly mean daily irradiation to monthly totals using calendar-day counts, summed to annual totals, and averaged over 2014–2023 [17]. The performance ratio, lifetime, degradation rate, and temporal aggregation procedure are model assumptions rather than parameters supplied by NASA POWER.

**Table 2.** Main data sources used in the screening model.

| Dataset | Publisher/year | Use in this study | Source |
|---|---|---|---|
| PV LCI report and spreadsheet | IEA PVPS Task 12, 2020 | Module BOM, foreground process electricity, and boundary interpretation | [4, 5] |
| Material factors | ecoinvent 3.9.1, 2022 | Thirteen material emission factors under the Cutoff system model and IPCC 2021 GWP100 | [10] |
| Power $CO_2$ factors | Ministry of Ecology and Environment and National Bureau of Statistics, 2025 | 2023 national and provincial electricity emission factors | [16] |
| Solar irradiation | NASA POWER, 2014–2023 | Monthly irradiation for 31 representative provincial cities | [17] |
| Technology-route proxies | ITRPV 2024 roadmap | Module efficiency, wafer thickness, silicon use, silver use, and general module-degradation trends used to construct route-specific proxies | [18] |

The data quality was qualitatively assessed using temporal, geographic, technological, precision, completeness, representativeness, consistency, reproducibility, and uncertainty criteria. Under this qualitative rating, 10 of the 13 ecoinvent material factors were assigned to the highest reliability category. Aluminium alloy frame and generic silicone are medium-reliability proxies, and aluminium paste is only represented by its primary aluminium component and is therefore a low-reliability proxy. Some background processes are Rest of World (RoW) or global market averages and should not be interpreted as measured inventories from Chinese suppliers. The full material-factor table, factor-replacement audit, and proxy ratings are supplied with the code package.

### 2.3. Carbon-footprint calculation

The cradle-to-gate carbon footprint per square metre is calculated as follows:

$$CF_{m^2} = \sum_i M_i EF_i + \sum_j E_j EF_{grid}, \tag{2.1}$$

where $M_i$ is the material use per square metre, $EF_i$ is the material emission factor, $E_j$ is foreground process electricity, and $EF_{grid}$ is the electricity $CO_2$ emission factor. Therefore, Eq (2.1) combines the material-side and foreground-electricity contributions on the common 1 $m^2$ basis. The baseline material factors are ecoinvent 3.9.1 Cutoff factors characterized with IPCC 2021 GWP100 [10]; $EF_{grid}$ is taken from the national or provincial 2023 electricity factors [16].

The footprint per installed capacity is as follows:

$$CF_{kWp} = \frac{CF_{m^2}}{\eta}, \tag{2.2}$$

where $\eta$ is the module power density in kWp/$m^2$. Equation 2.2 converts the area-based result to the installed-capacity functional unit. For the generic reference module, $\eta = 0.195$ kWp/$m^2$.

### 2.4. Lifetime generation and generation carbon intensity

For each representative city, the first-year electricity yield per kWp is estimated from NASA POWER horizontal global irradiation:

$$Y_1 = H \cdot PR, \tag{2.3}$$

where $H$ is the annual horizontal irradiation in kWh/$m^2$/year, and $PR$ is the performance ratio. Equation (2.3) is only used for the generation-denominator calculation. The screening model uses $PR = 0.80$. The lifetime generation per kWp is as follows:

$$G_{life} = Y_1 \sum_{t=0}^{T-1} (1-d)^t, \tag{2.4}$$

where $T = 25$ years, and the annual degradation rate is $d = 0.45\%$. Equation (2.4) applies the assumed degradation to the annual yield. Then, the manufacturing-attributed generation carbon intensity is as follows:

$$CI = \frac{CF_{kWp} \times 1000}{G_{life}}, \tag{2.5}$$

with units of g $CO_2$e/kWh. Equation 2.5 only allocates the modeled module manufacturing burden over the lifetime output. Horizontal irradiation is appropriate for province-level screening, but it does not include optimum tilt, shading, or site-specific power-plant design.

### 2.5. Scenario design

The scenario analysis varies three dimensions: manufacturing electricity and module efficiency, material-factor provenance, and technology route. For the manufacturing electricity and efficiency, the reference case uses the national-average electricity and 19.5% efficiency; green-electricity substitution

is only applied to the foreground process electricity, and the efficiency is varied to test how material and process burdens per kWp decline as the power density increases.

For the material-factor provenance, the ecoinvent scenario uses factors calculated in openLCA using licensed ecoinvent 3.9.1 Cutoff datasets and characterized with IPCC 2021 GWP100. The China-adjusted scenario uses literature and engineering proxies to represent a higher-carbon Chinese material supply assumption. The low-carbon scenario combines low-carbon silicon, a low-carbon aluminium-factor proxy, low-carbon glass, other low-carbon materials, and a high share of manufacturing green electricity. The China-adjusted and low-carbon factor sets are scenario proxies, not supplier-specific inventories or certified product declarations; they are used to test whether conclusions are driven by material-factor provenance. In the low-carbon scenario, the aluminium emission factor is 0.52 kg $CO_2$e/kg; this factor represents the modeled GWP100 per kilogram of aluminium input and is used as a screening proxy based on IAI-reported gate-to-gate emissions from aluminium-scrap processing [19]. This proxy excludes burdens embodied in the scrap and is applied without an explicit recycled-content share or scrap-allocation model; therefore, it should not be interpreted as a complete cradle-to-gate recycled-aluminium footprint. The low-carbon-silicon factor is treated as a historical, plant-specific screening proxy based on the A1–A3 result reported in the REC Solar Norway EPD [20], rather than as a current Chinese or global-average factor. The green-electricity substitution is modeled as a zero-carbon foreground process-electricity scenario and should not be interpreted as evidence of market-based procurement or physical electricity supply.

For the technology-route comparison, PERC, TOPCon, and HJT modules use roadmap-informed proxies for module efficiency, silicon intensity informed by wafer-thickness trends, silver use, and general module-degradation trends [18]. Route-specific process-energy scaling, degradation-rate differentiation, and other material-scaling factors are screening-level engineering assumptions, with the exact values documented in the accompanying reproducibility package.

Table 3 summarizes the factor, efficiency, electricity, and technology-route scenarios used in the analysis.

**Table 3.** Scenario definitions and interpretation boundaries.

| Scenario family | Material / technology setting | Electricity or efficiency setting | Interpretation boundary |
|---|---|---|---|
| Reference module | 19.5% generic c-Si module; IEA PVPS BOM and process energy | National-average or provincial foreground grid factor | Baseline manufacturing and production/use comparison |
| Ecoinvent Cutoff | Ecoinvent 3.9.1 Cutoff factors; PERC, TOPCon, or HJT route proxy | Route-specific efficiency and process-energy assumptions | Database-based screening comparison |
| China-adjusted | Higher-carbon literature and engineering material proxies | Same route-specific settings | Factor-provenance stress test, not a supplier inventory |
| Low-carbon | Low-carbon silicon, aluminium, glass, and other material proxies | High foreground green-electricity share | Combined material-and-foreground-power stress test |
| Efficiency / green electricity | Reference-module BOM held as the material object | Efficiency 19.5%–24.5%; foreground green electricity 0%–100% | Counterfactual sensitivity; green electricity is applied to foreground process electricity only |

### *2.6. Uncertainty and sensitivity analysis*

Input uncertainty is propagated to manufacturing footprints with Monte Carlo sampling. The material emission factors are perturbed by material-specific lognormal terms:

$$EF_i^* = EF_i \exp(\sigma_i Z), \qquad Z \sim N(0,1) \tag{2.6}$$

where $\sigma_i = \ln(\mathrm{GSD}_i)$. Equation (2.6) defines the factor perturbation used in the Monte Carlo analysis. The ecoinvent baseline uses GSD = 1.18, and the China-adjusted and low-carbon scenarios use GSD = 1.28 to reflect an additional scenario and proxy uncertainty. Solar-grade silicon, PV glass, and silver paste receive an additional 0.10 increment in GSD because they are high-impact or high-uncertainty inputs. Material amounts are lognormally perturbed with $\sigma = 0.06$, process-energy scale with $\sigma = 0.08$, module efficiency with a truncated normal standard deviation of 0.006, and electricity factors with a truncated relative normal standard deviation equal to 6% of the mean. Each technology-route/material-factor combination is sampled 20,000 times with independent random streams. The results are reported as P5, P50, and P95. These distributional settings are screening assumptions informed by common LCA uncertainty practice rather than measured supplier uncertainty distributions [15]. The numerical settings required to reproduce the Monte Carlo sampling and the generation-intensity propagation are summarized in Table 4.

Generation-intensity uncertainty is propagated separately from the material-side Monte Carlo. The manufacturing footprint uses an aggregate lognormal perturbation with GSD = 1.19, solar irradiation uses GSD = 1.04, performance ratio is sampled as 0.80 ± 0.03 truncated to 0.60–0.95, and the annual degradation rate is sampled as 0.45% ± 0.08% truncated to 0%–2%. A one-at-a-time tornado analysis and Monte Carlo Spearman correlations are used to identify the leading inputs for the ecoinvent PERC case.

**Table 4.** Computational parameters required to reproduce the Monte Carlo simulations and generation-intensity uncertainty analysis.

| Parameter | Setting / symbol | Value |
|---|---|---|
| Monte Carlo samples per technology-route–material-factor combination | $n$ | 20,000 |
| Random-number generator | – | PCG64, independent streams |
| Base seed, manufacturing-footprint Monte Carlo | seed | 42 |
| Seed, generation-intensity uncertainty | seed | 20240725 |
| Baseline GSD, ecoinvent 3.9.1 Cutoff scenario | GSD | 1.18 |
| Scenario GSD, China-adjusted and low-carbon scenarios | GSD | 1.28 |
| Additional GSD increment, solar-grade silicon, PV glass, silver paste | ΔGSD | 0.10 |
| Material-amount perturbation SD | $\sigma_M$ | 0.06 |
| Process-energy scale SD | $\sigma_E$ | 0.08 |
| Module-efficiency SD (truncated normal) | $\sigma_\eta$ | 0.006 |
| Electricity-factor relative SD (truncated normal) | $\sigma_{\text{grid}}$ | 0.06 |
| Aggregate manufacturing-footprint GSD, generation-intensity stage | $\text{GSD}_{\text{MC}}$ | 1.19 |
| Solar-resource GSD, generation-intensity stage | $\text{GSD}_{\text{solar}}$ | 1.04 |
| Performance ratio | PR | 0.80 (±0.03) |
| Annual degradation rate | $d$ | 0.45% (±0.08%) |
| Project lifetime | $T$ | 25 years |

## 3. Results

### *3.1. Overview of coupled LCA results*

The coupled results show that the interpretation of a module footprint changes when manufacturing emissions are allocated over lifetime generation. Figure 2 summarizes three model outputs: Panel A compares the deterministic route-specific footprints under the three factor sets, Panel B presents the corresponding Monte Carlo P5–P95 intervals, and Panel C shows selected same-province manufacturing-attributed generation carbon intensities. Together, the panels distinguish the effects of the material-factor provenance, technology route, and use-location solar resource.

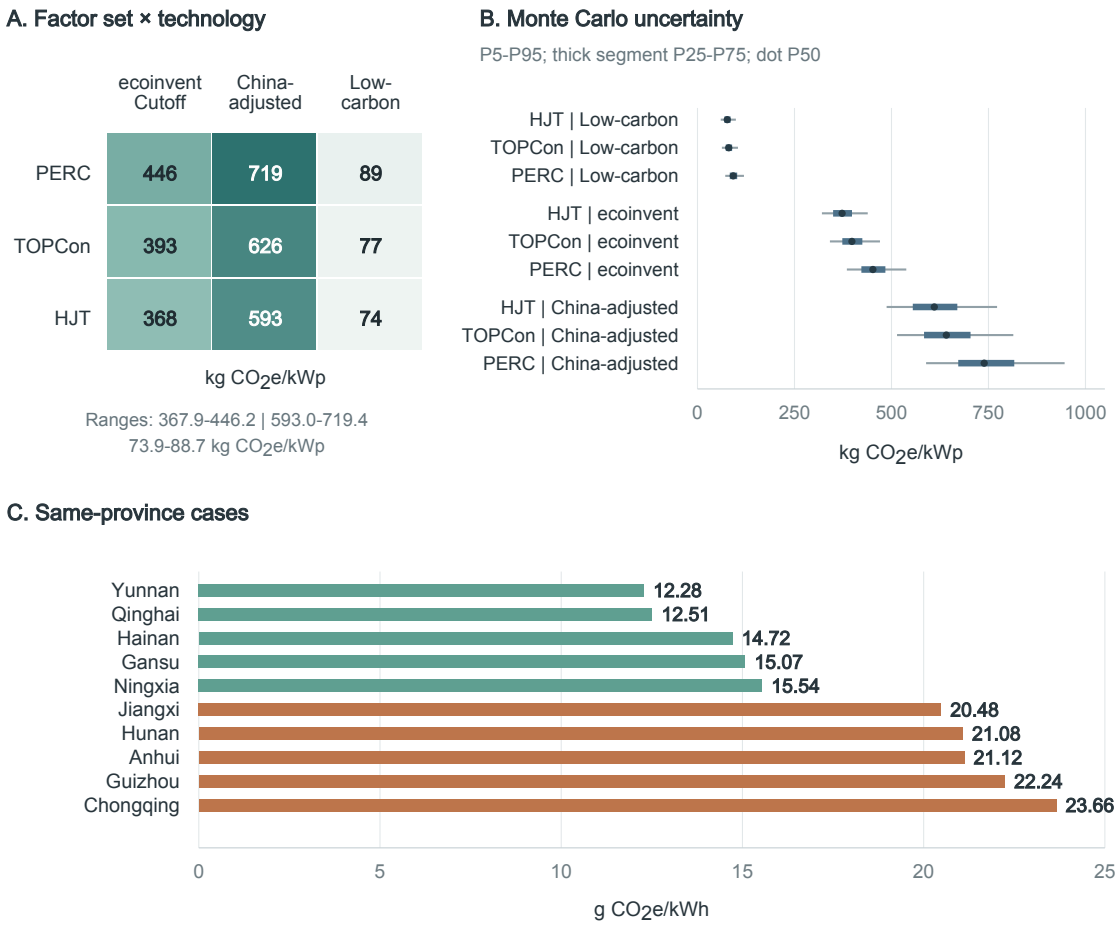



**Figure 2.** Overview of monocrystalline silicon photovoltaic module results. The panels summarize route-specific deterministic footprints (kg $CO_2$e/kWp), Monte Carlo P5–P95 intervals (kg $CO_2$e/kWp), and same-province manufacturing-attributed generation intensities (g $CO_2$e/kWh).

### *3.2. Manufacturing carbon footprints and hotspot contributions*

For the 19.5% reference module, the provincial manufacturing electricity changes the cradle-to-gate numerator before any solar-resource term is applied. The national-average manufacturing footprint is 494.4 kg $CO_2$e/kWp. Low-electricity-factor provinces have lower cradle-to-gate results: Yunnan and Sichuan reach about 385.6 and 391.9 kg $CO_2$e/kWp, respectively; and Jiangsu, Xinjiang, and Inner Mongolia reach about 508.6, 514.0, and 526.5 kg $CO_2$e/kWp, respectively. These differences arise from the foreground electricity term in Eq (2.1); without the manufacturing location, the footprint cannot be consistently interpreted.

Table 5 decomposes the baseline cradle-to-gate footprint of the 19.5% reference module into material and foreground-process-electricity contributions per unit area and per installed kilowatt-peak. The baseline material-side contribution is 68.08 kg $CO_2$e/m$^2$. Solar-grade silicon is the largest material contributor at 31.83 kg $CO_2$e/m$^2$ (163.2 kg $CO_2$e/kWp), followed by an aluminium alloy frame at 16.43 kg $CO_2$e/m$^2$ (84.2 kg $CO_2$e/kWp) and low-iron PV glass at

9.90 kg $CO_2$e/m$^2$ (50.8 kg $CO_2$e/kWp). Previous module-level research has highlighted aluminium frames as an important contributor [6]; the different hotspot ordering in the present model likely reflects differences in the module bill of materials, system boundary, background datasets, electricity assumptions, and aluminium-allocation approach. The foreground process electricity totals 53.38 kWh/m$^2$; at the national electricity factor, it contributes 28.32 kg $CO_2$e/m$^2$. In that foreground electricity, ingot pulling, cell manufacturing, and module encapsulation are the major terms.

**Table 5.** Baseline manufacturing contributions for the 19.5% reference module; material amounts are reported per m$^2$ unless otherwise noted.

| Item | Amount per m$^2$ | kg $CO_2$e/m$^2$ | kg $CO_2$e/kWp |
|---|---|---|---|
| Solar-grade silicon | 0.5735 kg/m$^2$ | 31.83 | 163.2 |
| Aluminium alloy frame | 2.1250 kg/m$^2$ | 16.43 | 84.2 |
| Low-iron photovoltaic glass | 8.8125 kg/m$^2$ | 9.90 | 50.8 |
| EVA encapsulant | 0.8750 kg/m$^2$ | 2.74 | 14.0 |
| PVF backsheet film | 0.1119 kg/m$^2$ | 2.30 | 11.8 |
| Silver | 0.0033 kg/m$^2$ | 1.53 | 7.9 |
| Other materials | – | 3.36 | 17.2 |
| All materials | – | 68.08 | 349.1 |
| Foreground electricity | 53.38 kWh/m$^2$ | 28.32 | 145.3 |
| Total, national grid | – | 96.40 | 494.4 |

### *3.3. Solar resource heterogeneity and same-province generation intensity*

NASA POWER data show large variations in the representative-city solar resource. Lhasa has the highest estimated first-year yield at 1617.3 kWh/kWp/year, followed by Yinchuan, Hohhot, Xining, Kunming, and Lanzhou. Because the generation carbon intensity divides the manufacturing footprint by the lifetime electricity generation, both the manufacturing electricity and the solar resource affect the same-province result.

Table 6 reports selected low and high same-province results. Yunnan and Qinghai combine relatively low manufacturing footprints with favorable solar resource and reach 12.28 and 12.51 g $CO_2$e/kWh, respectively. Chongqing and Guizhou reach 23.66 and 22.24 g $CO_2$e/kWh, respectively, because a lower lifetime generation and/or higher manufacturing footprints increase the ratio. The P5–P95 intervals reflect the separate propagation of aggregate manufacturing, irradiation, performance-ratio, and degradation uncertainty.

**Table 6.** Selected low and high same-province production/use results for the 19.5% reference module. $Y_1$ is the first-year yield, $G_{life}$ is the lifetime generation, and CI is the manufacturing-attributed generation intensity.

| Province | kg $CO_2$e/kWp | $Y_1$ | $G_{life}$ | CI (P5–P95) |
|---|---|---|---|---|
| Yunnan | 385.6 | 1325.2 | 31401.9 | 12.28 (9.08–16.55) |
| Qinghai | 398.3 | 1343.8 | 31842.0 | 12.51 (9.31–16.92) |
| Hainan | 449.0 | 1287.2 | 30501.9 | 14.72 (10.94–19.91) |
| Gansu | 471.5 | 1320.2 | 31283.2 | 15.07 (11.14–20.31) |
| Chongqing | 501.9 | 895.3 | 21214.8 | 23.66 (17.53–31.95) |
| Guizhou | 504.7 | 957.8 | 22695.5 | 22.24 (16.52–30.17) |
| Anhui | 528.5 | 1056.1 | 25024.5 | 21.12 (15.65–28.46) |
| Hunan | 485.3 | 971.8 | 23027.7 | 21.08 (15.65–28.44) |

### *3.4. Production–use matrix*

The production–use matrix separates the manufacturing-location and use-location effects that are hidden in a single same-province value. The matrix has 30 production provinces and 31 use provinces, giving 930 combinations. The 31 use provinces include Tibet for solar-resource calculation, while Tibet is not used as a production origin because the provincial manufacturing electricity-factor dataset used here does not provide a production factor for Tibet.

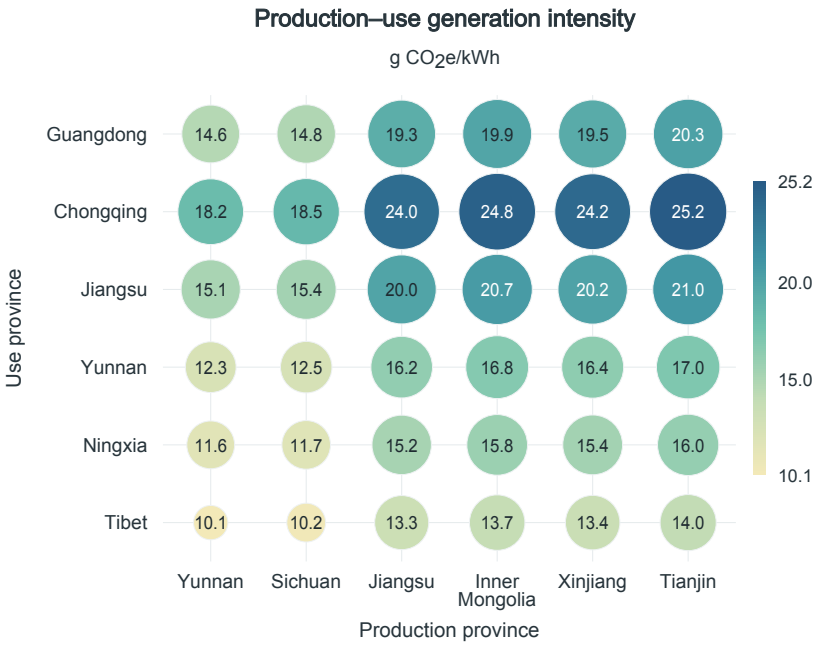



**Figure 3.** Representative 6 × 6 production–use submatrix of manufacturing-attributed generation intensity (g $CO_2$e/kWh), encoded by bubble color and area.

Figure 3 shows a representative 6 by 6 submatrix. The bubble color and area increase with the manufacturing-attributed generation intensity. The matrix distinguishes four cases: Low-carbon

manufacturing paired with high-resource use, low-carbon manufacturing paired with low-resource use, high-carbon manufacturing paired with high-resource use, and high-carbon manufacturing paired with low-resource use. A low factory-gate footprint does not necessarily yield the lowest g $CO_2$e/kWh if the module is used in a low-resource province. High use-location yield lowers the calculated intensity but does not remove the contribution of the production-province footprint.

### *3.5. Effects of efficiency, green electricity, material factors and technology routes*

Efficiency improvement lowers the material and process burden per kWp, while the foreground green-electricity substitution lowers process-electricity emissions. Efficiency enters because Eq (2.2) divides the area-based burden by the power density: with the BOM held on a per-area basis, a higher-efficiency module delivers more kWp from the same manufacturing burden. It does not reduce the carbon footprint per $m^2$ by itself. Under the national-average case, the 19.5% reference module without green electricity has a footprint of 494.4 kg $CO_2$e/kWp. Raising the efficiency to 24.5% and replacing all foreground process electricity with zero-carbon electricity lowers the footprint to 277.9 kg $CO_2$e/kWp, 56.2% of the reference value (Table 7 and Figure 4).

**Table 7.** Effect of module efficiency and foreground manufacturing green-electricity substitution under national-average electricity; footprints are reported as kg $CO_2$e/kWp.

| Module efficiency | Foreground green electricity | kg $CO_2$e/kWp |
|---|---|---|
| 19.5% | 0% | 494.4 |
| 19.5% | 50% | 421.8 |
| 19.5% | 100% | 349.1 |
| 23.0% | 0% | 419.1 |
| 23.0% | 50% | 357.6 |
| 23.0% | 100% | 296.0 |
| 24.5% | 0% | 393.5 |
| 24.5% | 50% | 335.7 |
| 24.5% | 100% | 277.9 |

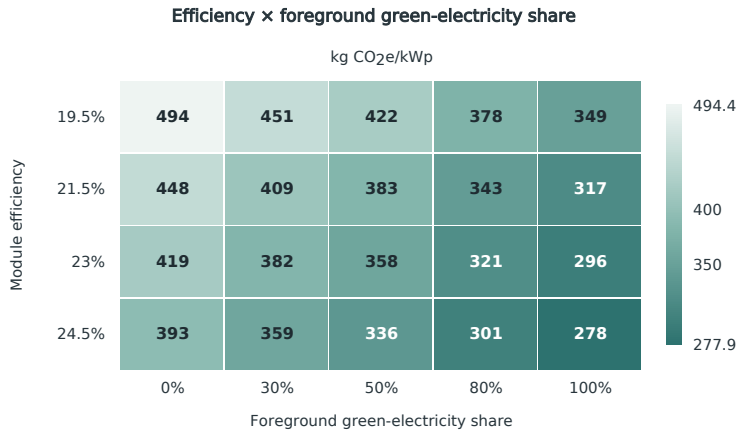



**Figure 4.** Manufacturing carbon footprint (kg $CO_2$e/kWp) under combinations of module efficiency and foreground manufacturing green-electricity share.

The route-specific values use the second module object in Table 1 and should be interpreted as route proxies rather than direct replacements for the 19.5% reference-module result. The route-specific results under the ecoinvent baseline are 446.2, 392.8, and 367.9 kg $CO_2$e/kWp for PERC, TOPCon, and HJT, respectively (Table 8). Under China-adjusted factors, the corresponding results are 719.4, 625.7, and 593.0 kg $CO_2$e/kWp, respectively. Under the low-carbon scenario, they decline to 88.7, 77.4, and 73.9 kg $CO_2$e/kWp, respectively. The green-electricity test is a foreground-process counterfactual: It does not replace the electricity used in upstream silicon, glass, aluminium, or other material supply chains. Therefore, it is not a claim that the entire supply chain is powered by low-carbon electricity, and it is not a comparison with switching coal to natural gas. The difference among factor scenarios is larger than the difference among technology routes within a given factor set.

**Table 8.** Deterministic results for route-specific PERC, TOPCon, and HJT module proxies under three material-factor scenarios. These values use the route-specific module object rather than the 19.5% reference module.

| Technology route | Factor scenario | Module efficiency | kg $CO_2$e/kWp |
|---|---|---|---|
| PERC | Ecoinvent 3.9.1 Cutoff | 20.5% | 446.2 |
| PERC | China-adjusted | 20.5% | 719.4 |
| PERC | Low-carbon | 20.5% | 88.7 |
| TOPCon | Ecoinvent 3.9.1 Cutoff | 22.8% | 392.8 |
| TOPCon | China-adjusted | 22.8% | 625.7 |
| TOPCon | Low-carbon | 22.8% | 77.4 |
| HJT | Ecoinvent 3.9.1 Cutoff | 23.5% | 367.9 |
| HJT | China-adjusted | 23.5% | 593.0 |
| HJT | Low-carbon | 23.5% | 73.9 |

### *3.6. Uncertainty, sensitivity and hotspot restructuring*

The Monte Carlo results are consistent with the deterministic comparison: the factor-scenario intervals are separated within each route, whereas the route intervals overlap within a factor set (Table 9). Within the same technology route, the ecoinvent P95 is below the China-adjusted P5, and the low-carbon P95 is below the ecoinvent P5. However, across technology routes, the intervals can overlap. For example, ecoinvent PERC has a P5–P95 range of 385.0–538.2 kg $CO_2$e/kWp, while ecoinvent TOPCon and HJT span 341.3–470.3 and 320.7–438.8 kg $CO_2$e/kWp, respectively. The P5–P95 intervals separate the material-factor scenarios within the same technology route, whereas PERC, TOPCon, and HJT intervals overlap within a given factor set. Therefore, route ranking is less stable than factor-scenario separation.

**Table 9.** Monte Carlo manufacturing carbon-footprint summary; P5, P50, and P95 are reported as kg $CO_2$e/kWp.

| Technology route | Factor scenario | P5 | P50 | P95 |
|---|---|---|---|---|
| PERC | Ecoinvent 3.9.1 Cutoff | 385.0 | 452.1 | 538.2 |
| PERC | China-adjusted | 589.2 | 738.9 | 946.2 |
| PERC | Low-carbon | 71.6 | 92.1 | 119.7 |
| TOPCon | Ecoinvent 3.9.1 Cutoff | 341.3 | 398.0 | 470.3 |
| TOPCon | China-adjusted | 514.3 | 641.3 | 814.0 |
| TOPCon | Low-carbon | 62.9 | 80.5 | 104.3 |
| HJT | Ecoinvent 3.9.1 Cutoff | 320.7 | 372.7 | 438.8 |
| HJT | China-adjusted | 487.4 | 610.4 | 772.1 |
| HJT | Low-carbon | 59.9 | 76.7 | 98.9 |

For the ecoinvent PERC case, the tornado analysis identifies the emission factor for solar-grade silicon as the most influential individual input. Varying this factor from its P5 to P95 value changes the footprint from approximately 398 to 519 kg $CO_2$e/kWp. The next most influential inputs are the module efficiency, the aluminium-frame emission factor, the PV glass emission factor, the process-energy scale, and the manufacturing-grid emission factor (Figure 5). Spearman correlations from the Monte Carlo input vector support the same ordering: the silicon factor has $\rho \approx 0.77$, the efficiency has $\rho \approx -0.28$, the aluminium frame has $\rho \approx 0.27$, and glass has $\rho \approx 0.25$. The reconstructed deterministic model used for the tornado analysis reproduces the nine deterministic technology-route/factor-scenario results to numerical precision.

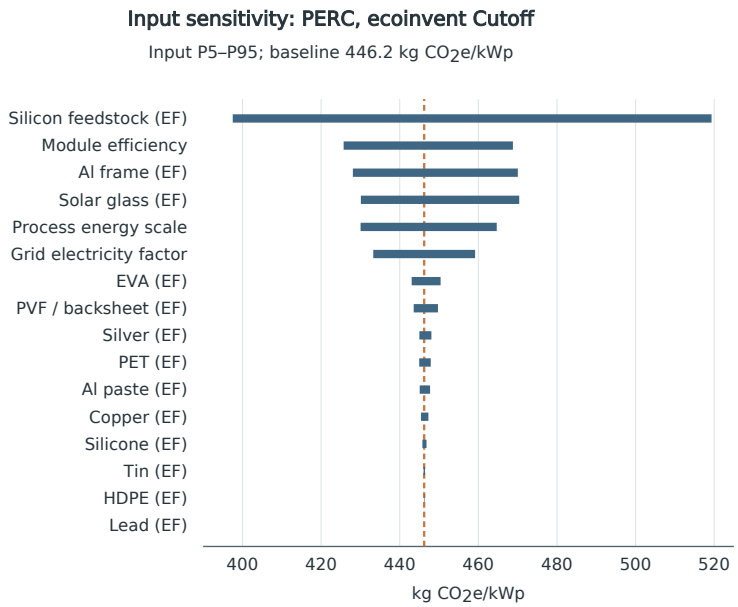



**Figure 5.** Input-level tornado analysis for the ecoinvent 3.9.1 PERC case. Bars show the change in the manufacturing carbon footprint (kg $CO_2$e/kWp) when each input moves from its own P5 to P95 while other inputs remain at deterministic values.

Additionally, the hotspot structure changes with the material-factor scenario and technology route (Figure 6). The solar-grade silicon, aluminium frame, and PV glass dominate the material side in the ecoinvent baseline. The China-adjusted scenario raises the contributions of silicon, aluminium, and glass. In the low-carbon scenario, these traditional hotspots are reduced and silver and other materials take a larger relative share. In this model, the low-carbon design gains are largest when the material substitution, material reduction, technology-route changes, and manufacturing electricity procurement are combined.

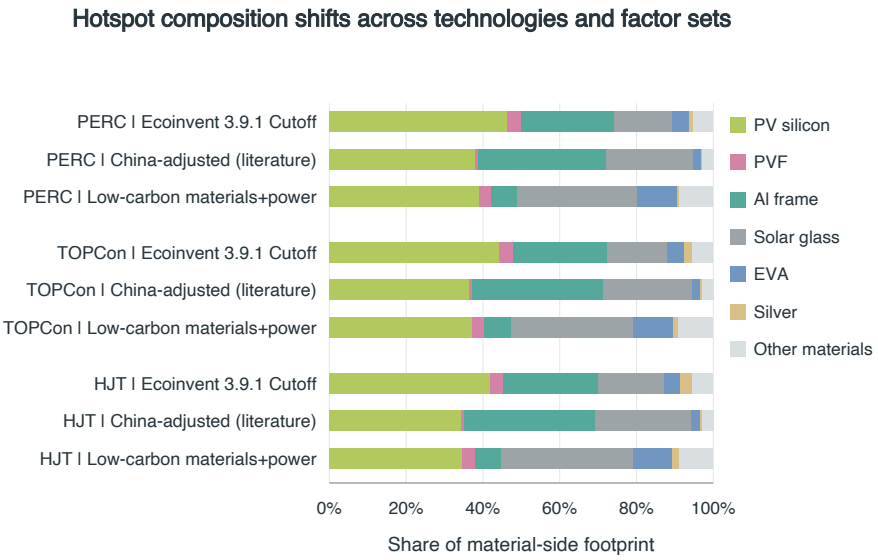



**Figure 6.** Material-side hotspot shares across technology routes and material-factor scenarios; the foreground process electricity is excluded from these shares.

### *3.7. Decarbonization pathway*

The waterfall scenario starts from China-adjusted PERC at 719.4 kg $CO_2$e/kWp (Figure 7). Switching to TOPCon and HJT lowers the footprint to 625.7 and 593.0 kg $CO_2$e/kWp, respectively. Then, the low-carbon silicon, low-carbon aluminium-factor proxy, and low-carbon glass reduce the result to about 449, 283, and 184 kg $CO_2$e/kWp, respectively. Other low-carbon materials lower it to about 172 kg $CO_2$e/kWp, and a 90% foreground green-electricity substitution gives a final value of 73.9 kg $CO_2$e/kWp. Technology-route upgrades provide efficiency and material-intensity benefits, but the largest step changes in this scenario occur after substituting silicon, aluminium, glass, and foreground electricity assumptions.

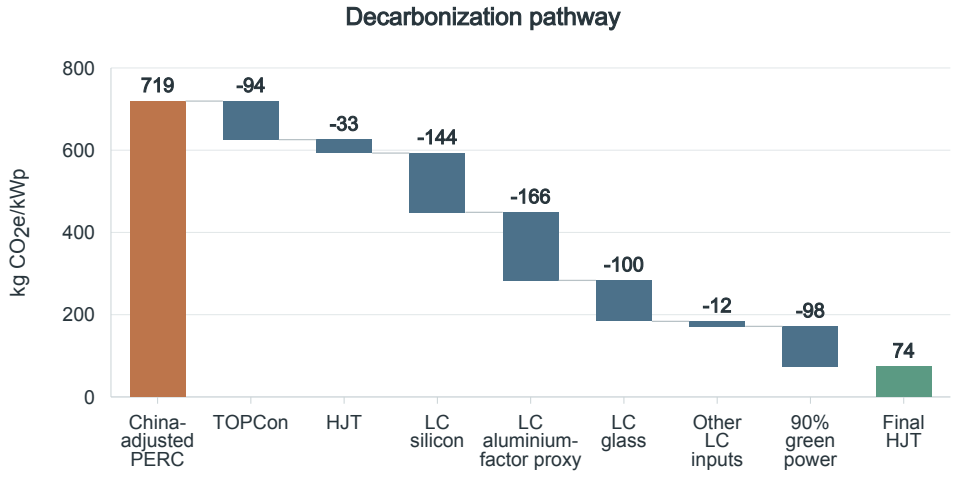



**Figure 7.** Illustrative scenario sequence from China-adjusted PERC to low-carbon HJT, reported in kg $CO_2$e/kWp. "Low-carbon aluminium-factor proxy" denotes the screening-level GWP100 factor per kilogram of aluminium input defined in Section 2.5.

## 4. Discussion

### *4.1. Regional implications of production–use coupling*

The main environmental implication is that the factory-gate footprint does not fully describe the module-manufacturing burden per generated kilowatt-hour. The manufacturing electricity changes the numerator, while use-location irradiation changes the lifetime-generation denominator. In the same-province cases, Yunnan and Qinghai are near 12.3–12.5 g $CO_2$e/kWh, whereas Chongqing and Guizhou are above 22 g $CO_2$e/kWh under the same screening boundary. Therefore, the production–use matrix describes a pairing problem rather than a single province ranking. It separates two conditions that are often collapsed in product-footprint summaries: low factory-gate footprint and high use-location lifetime generation. This separation is relevant for product carbon-footprint disclosure, low-carbon procurement, and regional supply-chain decisions because each decision uses a different part of the calculation.

### *4.2. Data-source choice and carbon-footprint comparability*

For this screening boundary, the material-factor provenance changes the absolute footprint more than the cell-route choice does. These reporting choices affect the interpretation because the database version, system model, LCIA method, geographic proxy, reference product, and recycled-material rule can shift both total footprints and hotspot rankings. The China-adjusted case is an author-defined high-carbon screening scenario, while the low-carbon case combines two literature-based proxies with additional author-defined material and electricity assumptions. Neither scenario should be read as a measured or harmonized supplier inventory; rather, they quantify the sensitivity to factor provenance within the tested assumptions. Geographic-representativeness concerns for modules manufactured in

China were discussed by Mariutti [11], while research on Mexican module production illustrated the effects of globally distributed supply chains, imported cells, and transport [14]. Public silicon-PV LCI data gaps are documented by Rodriguez Garcia and Kneifel [12].

For comparison, Müller et al. [7] reported approximately 750 and 810 kg $CO_2$e/kWp for glass-glass and glass-backsheet modules produced in China, respectively, while Mariutti [11] summarized manufacturer-EPD values of approximately 395–460 kg $CO_2$e/kWp. The present ecoinvent-based results of 367.9–494.4 kg $CO_2$e/kWp overlap with the latter range but are lower than the values reported by Müller et al. These differences may reflect variations in the module design, efficiency, manufacturing electricity, system boundary, and background inventory; therefore, the comparison should be interpreted as indicative rather than fully harmonized. Additionally, this comparison underscores that the object being modeled matters: cell-production hotspots cannot be directly equated with a framed module because glass, encapsulants, frames, and module-assembly burdens enter the module functional unit.

Compared with the EPEAT embodied-carbon reference thresholds of 630 kg $CO_2$e/kWp for required Low Carbon Solar and 400 kg $CO_2$e/kWp for optional Ultra-Low Carbon Solar [21], the calculated ecoinvent-baseline values for PERC, TOPCon, and HJT are numerically below 630 kg $CO_2$e/kWp, while the TOPCon and HJT values are also numerically below 400 kg $CO_2$e/kWp. These numerical comparisons do not demonstrate EPEAT conformance because the present screening model does not apply the complete the Verified Carbon Footprint method or the required independent third-party verification procedure. Under China-adjusted factors, PERC exceeds 630 kg $CO_2$e/kWp, while TOPCon and HJT remain close to or below that value. Under the low-carbon scenario assumptions, all three routes are 73.9–88.7 kg $CO_2$e/kWp. Therefore, the threshold comparison is conditional on the cradle-to-gate module boundary and the selected factor set; it should not be interpreted as external certification.

### *4.3. Relation to technology evolution and hotspot literature*

The direction of the technology-route results is consistent with work showing that higher efficiency and lower material intensity reduce crystalline-silicon module burdens over time [8, 9]. However, the overlap among PERC, TOPCon, and HJT uncertainty intervals cautions against reading a public-roadmap route proxy as a product-specific claim. For supplier declarations, measured BOMs, EPDs, electricity procurement evidence, and authorized background databases are needed. The hotspot results also agree with IEA PVPS inventory interpretation: silicon, glass, aluminium, and manufacturing electricity remain central drivers [4]. This study adds a production–use geographic perspective to these established hotspot categories and examines how their interpretation changes across material-factor scenarios.

### *4.4. Limitations and future work*

Several limitations follow from the screening goal. First, several materials use RoW or global-market ecoinvent background processes, while the foreground process electricity uses Chinese provincial factors. The resulting boundary is transparent but geographically mixed. Authorized databases or supplier measurements should replace the proxy factors before product-specific comparative claims are made; this is a limitation of the present screening analysis rather than a

further method assumption. Second, NASA POWER horizontal irradiation supports province-level comparison but omits optimum tilt, site design, local shading, and plant-level performance. Using plane-of-array irradiation would increase the modeled lifetime generation for many fixed-tilt systems and would therefore lower the absolute g $CO_2$e/kWh values, although the direction and magnitude would vary by location and system design. Third, transport, mounting structures, inverters, operation and maintenance, and end-of-life processes are outside the baseline boundary. Here, transport refers to module-level transport and other foreground logistics not already embedded in selected ecoinvent market or production datasets. IEA PVPS inventories show that balance-of-system components and operational inputs form part of complete PV-system inventories and can affect the system-level LCA results. Additionally, the end-of-life results depend on the selected treatment, disposal, and recycling pathways [22]. Therefore, these processes should be included before complete power-plant life-cycle claims are made. Fourth, the Monte Carlo inputs are treated as independent, the aggregate generation-intensity uncertainty uses an approximation to the manufacturing-footprint uncertainty, the provincial grid-factor method uncertainty is not fully propagated, and the qualitative reliability ratings are not converted into a formal pedigree matrix. For public comparative assertions between products, ISO 14044 critical-review requirements and supplier-specific data should be applied.

## 5. Conclusions

The main takeaway is that a PV module carbon footprint should not be reported as a single number detached from its manufacturing location, material-factor provenance, and use-location solar resource. This screening assessment couples module manufacturing inventories, provincial electricity factors, long-term solar resource, material-factor scenarios, and technology-route assumptions. For the 19.5% reference module, the national-average manufacturing footprint is 494.4 kg $CO_2$e/kWp. When that cradle-to-gate burden is allocated over same-province lifetime generation, selected low-intensity cases such as Yunnan and Qinghai reach 12.28 and 12.51 g $CO_2$e/kWh, respectively, while selected high-intensity cases such as Chongqing and Guizhou reach 23.66 and 22.24 g $CO_2$e/kWh, respectively.

The production–use matrix shows that low factory-gate footprint and high lifetime generation are separate conditions and should be reported together. The material-factor comparison further shows that factor provenance can shift footprints more than the route difference among PERC, TOPCon, and HJT within this model. Under ecoinvent factors, route-specific results are 446.2, 392.8, and 367.9 kg $CO_2$e/kWp, respectively, whereas China-adjusted factors raise them to 593.0–719.4 kg $CO_2$e/kWp and the low-carbon scenario reduces them to 73.9–88.7 kg $CO_2$e/kWp.

For the product carbon-footprint reporting, the material database, system model, LCIA method, geographic proxy, technology-route parameters, and manufacturing electricity should be disclosed alongside the numerical footprint. Efficiency improvement reduces the per-kWp burden, but the largest step changes in the tested scenario sequence occur after substituting silicon, aluminium, glass, and foreground electricity assumptions. Future work should replace the proxy factors with supplier BOMs, EPDs, authorized databases, plant-specific electricity data, and complete balance-of-system and end-of-life inventories before comparative public claims are made.

## Use of AI tools declaration

The authors declare that ChatGPT 5.5 was used to assist with Chinese-to-English translation. The authors reviewed all content and are fully responsible for the manuscript.

## Acknowledgments

This work was supported by Zhejiang Key Laboratory of Film and TV Media Technology No. 2024E10023 and Natural Science Foundation of China No. 61671404.

## Conflict of interest

The authors declare no conflict of interest.

## Data availability

The analysis code, fixed input tables, lcpy source snapshot, reference numerical outputs, and reference figure set are available at https://github.com/hipovel/single-si-pv-lca.

## References

1. International Organization for Standardization (2006) ISO 14040: Environmental management–life cycle assessment–principles and framework. Available from: https://www.iso.org/standard/37456.html.
2. International Organization for Standardization (2006) ISO 14044: Environmental management–life cycle assessment–requirements and guidelines. Available from: https://www.iso.org/standard/38498.html.
3. International Organization for Standardization (2018) ISO 14067: Greenhouse gases–carbon footprint of products–requirements and guidelines for quantification. Available from: https://www.iso.org/standard/71206.html.
4. IEA PVPS Task 12 (2020) Life cycle inventories and life cycle assessments of photovoltaic systems. Available from: https://iea-pvps.org/key-topics/life-cycle-inventories-and-life-cycle-assessments-of-photovoltaic-systems/.
5. IEA PVPS Task 12 (2020) PV supply chain LCI spreadsheet. Available from: https://iea-pvps.org/wp-content/uploads/2020/12/PVPS-Task12-19_2020_EcoSpold_LCI-PV-supplyChains-CC-BY-NC-SA-4.0.xlsx.
6. Chowdhury P, Chowdhury H, Chowdhury T, et al. (2026) Standardization as a pathway to a circular PV industry: Addressing material recovery and design challenges. *Sol Energ Mat Sol C* 296: 114067. https://doi.org/10.1016/j.solmat.2025.114067
7. Müller A, Friedrich L, Reichel C, et al. (2021) A comparative life cycle assessment of silicon PV modules: Impact of module design, manufacturing location and inventory. *Sol Energ Mat Sol C* 230: 111277. https://doi.org/10.1016/j.solmat.2021.111277

8. Yuan L, Nain P, Kothari M, et al. (2024) Material intensity and carbon footprint of crystalline silicon module assembly over time. *Sol Energy* 269: 112336. https://doi.org/10.1016/j.solener.2024.112336
9. Louwen A, van Sark WGJHM, Faaij APC, et al. (2016) Re-assessment of net energy production and greenhouse gas emissions avoidance after 40 years of photovoltaics development. *Nat Commun* 7: 13728. https://doi.org/10.1038/ncomms13728
10. Wernet G, Bauer C, Steubing B, et al. (2016) The ecoinvent database version 3 (part I): Overview and methodology. *Int J Life Cycle Ass* 21: 1218–1230. https://doi.org/10.1007/s11367-016-1087-8
11. Mariutti E (2025) The limits of the current consensus regarding the carbon footprint of photovoltaic modules manufactured in China: A review and case study. *Energies* 18: 1178. https://doi.org/10.3390/en18051178
12. Garcia GR, Kneifel J (2025) Public life cycle inventory data gap analysis for silicon-based photovoltaic panels, NIST Technical Note 2350. https://doi.org/10.6028/NIST.TN.2350
13. Luo Z, Yu P, Wang H, et al. (2025) Life-cycle assessment of monocrystalline silicon photovoltaic systems. *Acta Energ Sol Sin* 46: 237–243. https://doi.org/10.19912/j.0254-0096.tynxb.2024-1022
14. Hernandez-Padilla F, Borja V, Urbina A (2026) Life cycle assessment of photovoltaic module production in Mexico: hidden impacts of global manufacturing. *Sustainability* 18: 175. https://doi.org/10.3390/su18010175
15. Michiels F, Geeraerd A (2022) Two-dimensional Monte Carlo simulations in LCA: An innovative approach to guide the choice for the environmentally preferable option. *Int J Life Cycle Ass* 27: 505–523. https://doi.org/10.1007/s11367-022-02041-0
16. Ministry of Ecology and Environment of the People's Republic of China, National Bureau of Statistics of China (2025) 2023 power carbon dioxide emission factors. Available from: https://www.mee.gov.cn/xxgk2018/xxgk/xxgk01/202512/W020251231726284332528.pdf.
17. NASA Langley Research Center (2026) POWER Data Access Viewer and API. Available from: https://power.larc.nasa.gov/api/pages/.
18. ITRPV (2024) International Technology Roadmap for Photovoltaic results 2024 presentation. Available from: https://solar-media.s3.amazonaws.com/assets/PVCellTechEurope24/20240313_ITRPV_15th_edition_presentation_PVCellTech_MF_240313.pdf.
19. International Aluminium Institute (n.d.) Aluminium recycling and greenhouse gas emissions. Available from: https://international-aluminium.org/landing/as-well-as-aluminium-recycling-saving-95-of-the-energy-needed-for-primary-aluminium-production-the-recycling-process-saves-a-similar-percentage-in-greenhouse-gas-emissions/.
20. REC Solar Norway AS (2021) Environmental Product Declaration: REC Solar solar grade silicon (SoG-Si), NEPD-2681-1371-EN. The Norwegian EPD Foundation. Available from: https://www.recgroup.com/sites/default/files/documents/nepd-2681-1371_rec-solar-solar-grade-silicon-sog-si-.pdf.

21. Global Electronics Council (2024) Criteria for the Assessment of Ultra-Low Carbon Solar Modules: EPEAT-ULCS-2023, Interim Corrections December 2024. Available from: https://globalelectronicscouncil.org/wp-content/uploads/EPEAT_ULCS_2023_Interim_Corrections-December_2024.pdf.

22. Singh S, Powar S, Dhar A (2023) End of life management of crystalline silicon and cadmium telluride photovoltaic modules utilising life cycle assessment. *Resour Conserv Recy* 197: 107097. https://doi.org/10.1016/j.resconrec.2023.107097




AIMS Press

© 2026 the Author(s), licensee AIMS Press. This is an open access article distributed under the terms of the Creative Commons Attribution License (https://creativecommons.org/licenses/by/4.0)